



## Influence of Vertical Loads on the Response of Laterally Loaded Piles In Medium Stiff Clay

**Fath Elrahman Eltayeb Nur Eldayem<sup>1</sup>, Abu Baker Abd Elwhab<sup>2</sup>, Yahia E-A. Mohamedzein<sup>3</sup>**

<sup>1</sup>*Civil Engineering Department, Faculty of Engineering, Alzaiem Alazhari University*

<sup>2</sup>*Civil Engineering Department, Faculty of Engineering, University of Khartoum*

<sup>3</sup>*Civil and Architectural Engineering Department, College of Engineering, Sultan Qaboos University  
Sultanate of Oman P.O. Box 33, Al-Khod 123*

**Abstract:** This paper investigates the influence of vertical loads on laterally loaded piles. It includes laboratory model tests of steel piles embedded in medium stiff clay and a parametric study. The laboratory tests were performed at the Faculty of Engineering, University of Khartoum in Sudan. The parametric study considers the effects of different values of the vertical load and the length-to-diameter (L/d) ratio of the pile on the pile behavior. The performance of pile considered will include the ultimate lateral capacity of pile, the pile head deflection, load-maximum moment curves and the shear force along the length of the pile.

### 1. INTRODUCTION

Piles are deep foundations that are used to support heavy loads structures. Piles are subjected to lateral loads as well as vertical loads. Lateral loads are due to winds, hurricanes, earthquakes ... etc. (Patra and Pise, 2001, Fan and Long, 2005). In the current practice piles are independently analyzed first for the vertical load to determine their bearing capacity and the settlement and for the lateral load to determine their flexural behavior. The behavior of vertically-loaded piles is investigated by many researches (Sorchan, 1980; Elsharief, A. M., 1987). The behavior of laterally-loaded piles was studied by Poulos and Davis (1980); Dunnivant et al. (1989); Sun (1994); Mayne et al. (1995); Briaud (1997); Reese (1997); Wu et. al. (1998); S. Rao et al. (1998); Patra and Pise (2001); Rajashree and Sitharam (2001); Gabr (2002); Yang and Jeremic (2002); Hsiung (2003); Kim et al. (2004); Küçükarslan and Banerjee (2004); Yang (2006) Ahmadi and Ahmari (2009) and few researchers considered the interaction effects between the vertical and lateral loads. The influence of the vertical load on the behavior of the laterally loaded piles was studied theoretically by Karasev et al., (1977); Karthigeyan et al., (2006) and experimentally by Bartolomey AA., (1977) and Anagnostopoulos C. et al., (1993).

The objective of this study is to consider the influence of the vertical load on the performance of laterally loaded piles in medium stiff clay and to predict the ultimate pile

capacity. The effects of length-to-diameter (L/d) ratio on the performance of the laterally loaded pile subjected to vertical load was also considered. The performance of pile considered will include the ultimate lateral capacity of pile, the pile head deflection, load-maximum moment curves and the shear force along the length of the pile.

### 2. Scope of the Study

Two laboratory model tests on steel piles of diameter of 31.1 mm and L/d ratio of 10 and 20 under vertical and lateral loads were performed. The finite element program (ABAQUS) has been used for the analysis of the laboratory model test and a typical steel pile in medium stiff clay. A parametric study for the effects of different vertical loads values and length-to-diameter (L/d) ratio on the laterally loaded piles with and without vertical load was also considered.

### 3. Experimental Program

#### 3.1 Test Setup and Instrumentation

The laboratory model tests were performed in a tank of 1000 mm wide, 1250 mm long and 1400 mm high. It was made of 3 mm thick steel plates. Each pile was instrumented with eight strain gauges of type FLA-10-11. The stain gauges were attached to the outside surface of the steel pile along its embedded length. Two TML displacement transducers type CDP-25B of 25 mm

travelling distance were used to measure the deflections of the pile at two different positions, at the soil surface and at 100 mm above the soil surface. A TDS303 data logger was used to monitor and record the readings of the strain gauges and the displacement transducers. Figure 1 presents strain gauges layout and the lateral load arrangements.

The pile alignment system during soil placements consists of two box sections made of double angles and steel rods. The loading frame consists of a reaction steel plate 10 mm thick and 200 mm wide fixed to a reinforced concrete column. A manual jack of 30 kN capacity was used to apply the horizontal loads to the pile. To monitor the actual applied load in the vertical and lateral directions, a calibrated proofing rings were placed between the loading points on the jacks and the pile. Figure 2 presents test setup and loading arrangements for vertical and lateral loads.

### 3.2 Test Procedure

Two models of steel piles of diameter of 31.1 mm and L/d=10 and 20 under vertical loads were performed. The steel piles were held, aligned and kept vertically in the centre of the test tank prior to the soil placement.

The clay soil was placed in layers of 200 mm and compacted to the required density. Compaction for each layer was done manually by using a weight of 30 kg. Compaction was continued for each layer until no reduction in the layer thickness would be observed and the required level was reached. By the completion of the soil placement, the clay surface was leveled and the loading was applied in two steps. Step 1: the vertical load was applied in increments until the end of the ultimate vertical load and step 2: the lateral load was applied while the vertical load was kept constant at its ultimate value. Then the readings of the strain gauges and the deflections were taken first for the vertical load alone and second for the lateral loads with the vertical load.

### 3.3 Analysis of Results

The behavior of the piles can be presented in terms of load-deflection curves at the pile head, load-maximum moment curves and the shear force along the length of the pile.

The governing differential equations to find the deflection (y), moment (M) and the shear force (V) along the length of the pile (Z) are:

$$y = \int(\int \phi \, dZ) \, dZ \quad (1)$$

$$M = EI \phi \quad (2)$$

$$dV = \frac{dM}{dz} \quad (3)$$

Where

$E I$  = modulus of rigidity of the pile.

$\phi$  = curvature of the pile shaft ( $\phi$  = difference between compression and tension strains measured at the same depth divided by the distance between these two strains). Figure 3 presents the vertical load-deflection curve for steel piles under vertical load only. The greater L/d ratio the greater vertical soil resistance to the pile. this phenomenon is physically acceptable because the frictional forces between the pile and the soil is increased with increasing the contact area relating to the increased L/d ratio.

The influence of vertical load on the response of laterally loaded pile was examined by analyzing a model steel pile of diameter 31.1 mm and L/d ratio=20. Two cases of loadings were performed. in the first case the pile was subjected to lateral load only (the vertical load  $V=0$  kN) and in the second case the pile was loaded vertically up to its ultimate vertical load ( $V=Vu$ ) then the lateral load was applied in increments. The ultimate vertical load was obtained at a vertical deflection of 0.1d. Figure 4 presents load-deflection curves for a model steel pile of diameter of 31.1 mm and L/d=20 with and without vertical load. It is seen from this figure the presence of the vertical load significantly decreases the lateral resistance of the pile. This result was also obtained by Karthigeyan et al., (2005).

Figure 5 presents load-maximum moment curves for the experimental models. These curves show a linear criteria for the case of presence of vertical load and nonlinear where there is no vertical load. The presence of the vertical load increases the bending moment in the pile and thus reduces the lateral resistance of the pile.

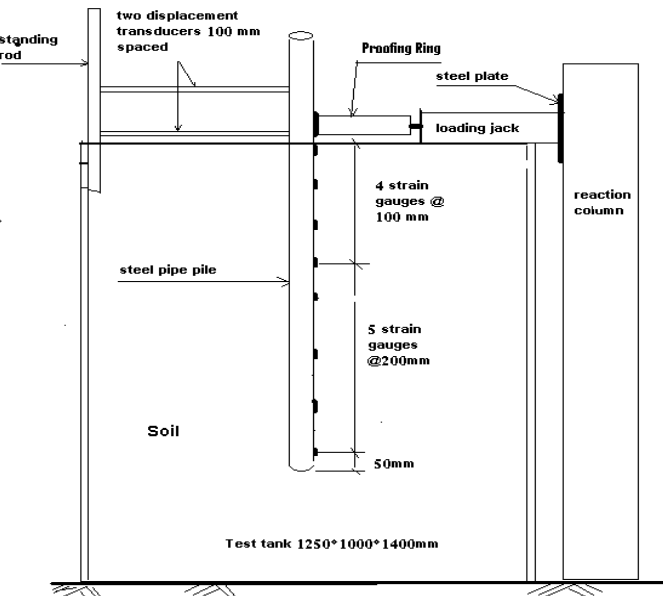


**Figure (1).** Strain gauges layout and the lateral load arrangements



**Figure (2).** Test setup and loading arrangements for vertical and lateral loading

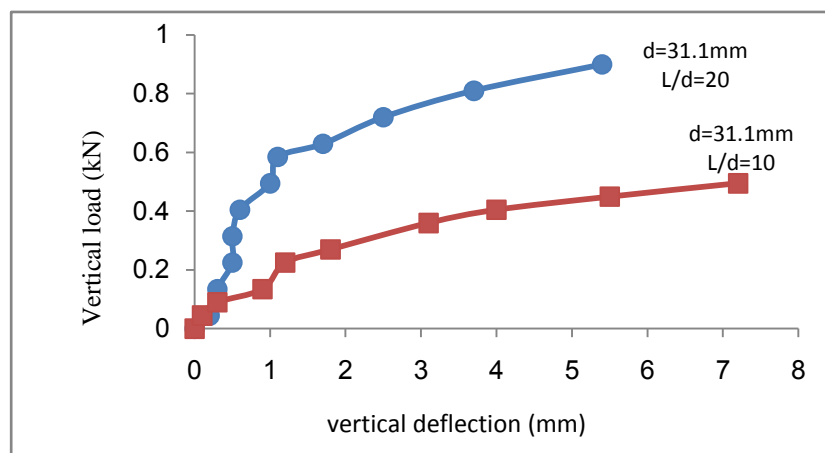


**Figure (3).** Load-deflection curves for steel Pile under vertical loads (Exp.)

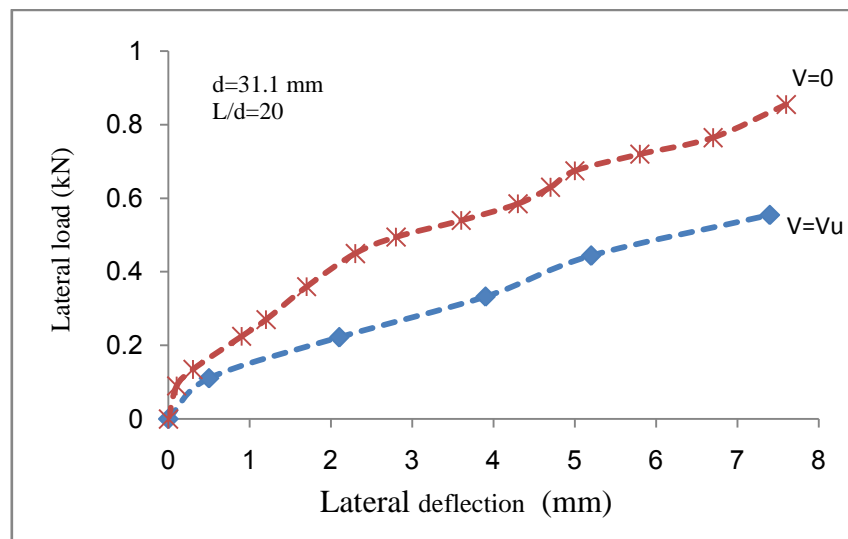


**Figure (4).** Load-deflection curves for steel pile under lateral loads with and without vertical load (Exp.)

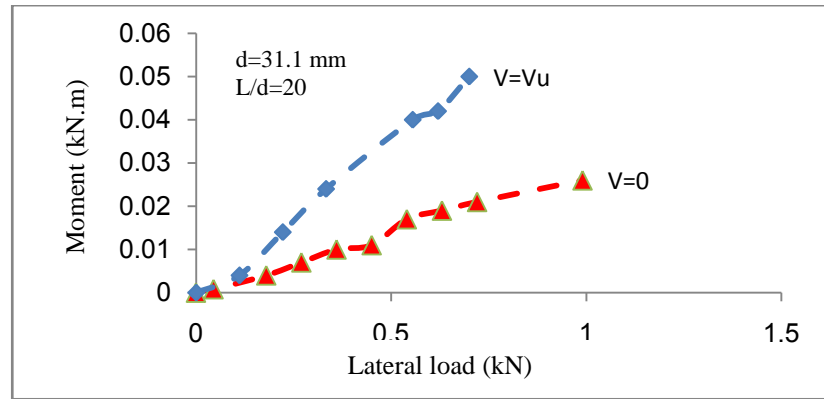


**Figure (5).** Load-maximum moment curves for steel pile with and without vertical load (Exp.)

#### 4. Numerical Model

ABAQUS program was used to analyze the pile-soil system. The main feature of the finite element model depended on the pile dimensions (length and diameter), the embedded length of the pile and the soil dimensions. In the case of modeling laboratory test piles, the dimensions of the test tank (1200 mm length, 1000 mm width and 1400 mm in height) were used to present the soil dimensions. A steel pile embedded in medium stiff clay was used. The pile behavior was modeled as linearly elastic defined by the material elastic modulus ( $E$ ) and the poison's ratio ( $\mu$ ). The soil material was presented by the Modified Drucker-Prager

model criteria for clay. Moreover the modeling of full-scale field tests was treated in the same manner linear elastic model for pile material and Modified Drucker-Prager model for the clay. An 8-node linear brick elements (C3D8) was adopted for both pile and the soil. The finite element mesh used for the soil was fine close to the pile and in the upper region of the soil close to the soil surface. Figure 6 presents the details of the pile-soil arrangement. Fixed boundary conditions at the bottom and at the soil sides were generated. Surface-to-surface interaction between the pile and the soil was used. The lateral load was applied to pile at a point close to the soil surface while the vertical load was applied as a concentric loading.

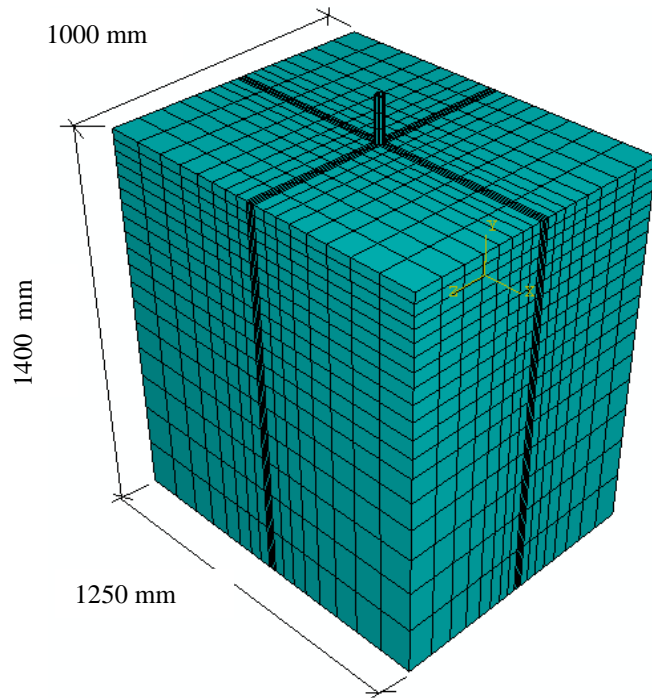


**Figure (6).** The finite element mesh for laboratory model test for a pile of diameter of 31.1 mm and  $L/d=20$

#### 4.1 Validation of the FF Model

The validity of the numerical model was verified by considering two different examples. The results of the FE model were compared with the results of the fore-mentioned laboratory model test and with the results of elastic solution for a laterally loaded pile. The numerical modeling for each example will be performed according to

The tested model steel pile was analyzed numerically using ABAQUS program. The pile length and diameter were 0.58 m and 0.058m, respectively. The pile is embedded in a homogeneous medium stiff clay. Table 1 presents the clay properties. The real size of the test tank and the pile were used to generate the finite element mesh. Comparison was carried between the load-deflection curves and moment-depth profiles.

Figure 7 presents the load-deflection curves for the laboratory test and the FE model results. Both curves have the same results up to a deflection of 0.1d (deflection at the

ABAQUS software feature. Description of the problem includes (1) different parts type, size and discretization, (2) materials properties, (3) element type and size, (4) assembly of the different parts and the interaction between them, (5) the process of analysis and finally (6) the output of the results.

##### 4.1.2 Comparison with Laboratory Model Test

ultimate load). Some deviations in the deflection curves took place beyond the point of the ultimate load. it is clear that the load-deflection curves for the laboratory model test and the FE model had similar trends.

Figures 8 and 9 present moment-depth profiles for the laboratory model test and the FE model. The point of maximum bending moment for the laboratory model test and the FE model occurred at a depth of 0.15 and 0.18 m, respectively. The FE model gave higher moment values than the laboratory model test but generally the two profiles had the same trend.

**Table (1).** properties of clay

property	value
Liquid limit (%)	50
Plastic limit (%)	25
Percentage passing sieve#200	97
Specific gravity	2.6
Optimum moisture content (%)	24.5
Maximum dry density (gm/cm <sup>3</sup> )	1.519
Undrained shear strength from unconfined compression (kN/m <sup>2</sup> )	17.5
Undrained shear strength friction angle from UU (degrees)	24
Undrained shear strength cohesion (c) from UU (kN/m <sup>2</sup> )	20
Undrained shear strength friction angle from CU (degrees)	21
Undrained shear strength cohesion (cu) from CU (kN/m <sup>2</sup> )	31
Compression coefficient of c <sub>c</sub>	0.2704
Recompression coefficient c <sub>r</sub>	0.04
Initial Young modulus from unconfined	2000-4500
Initial Young modulus from UU	4000-6500
Initial Young modulus from CU	3000-6000
Maximum past pre-consolidation pressure (kN/m <sup>2</sup> )	230

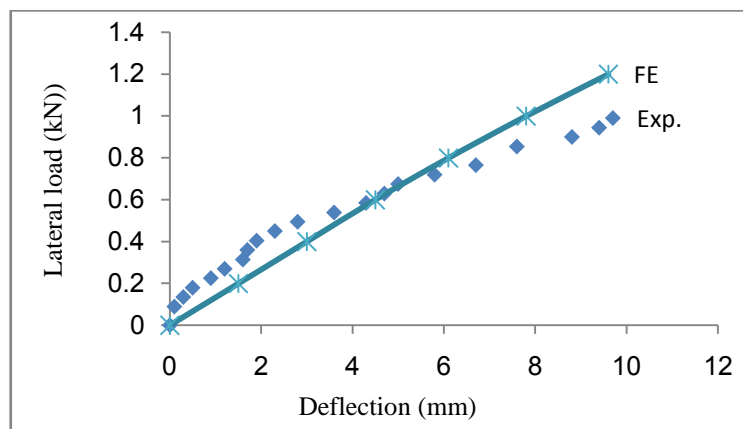


**Figure (7).** Load-deflection curves comparison for the laboratory model test and the FE model

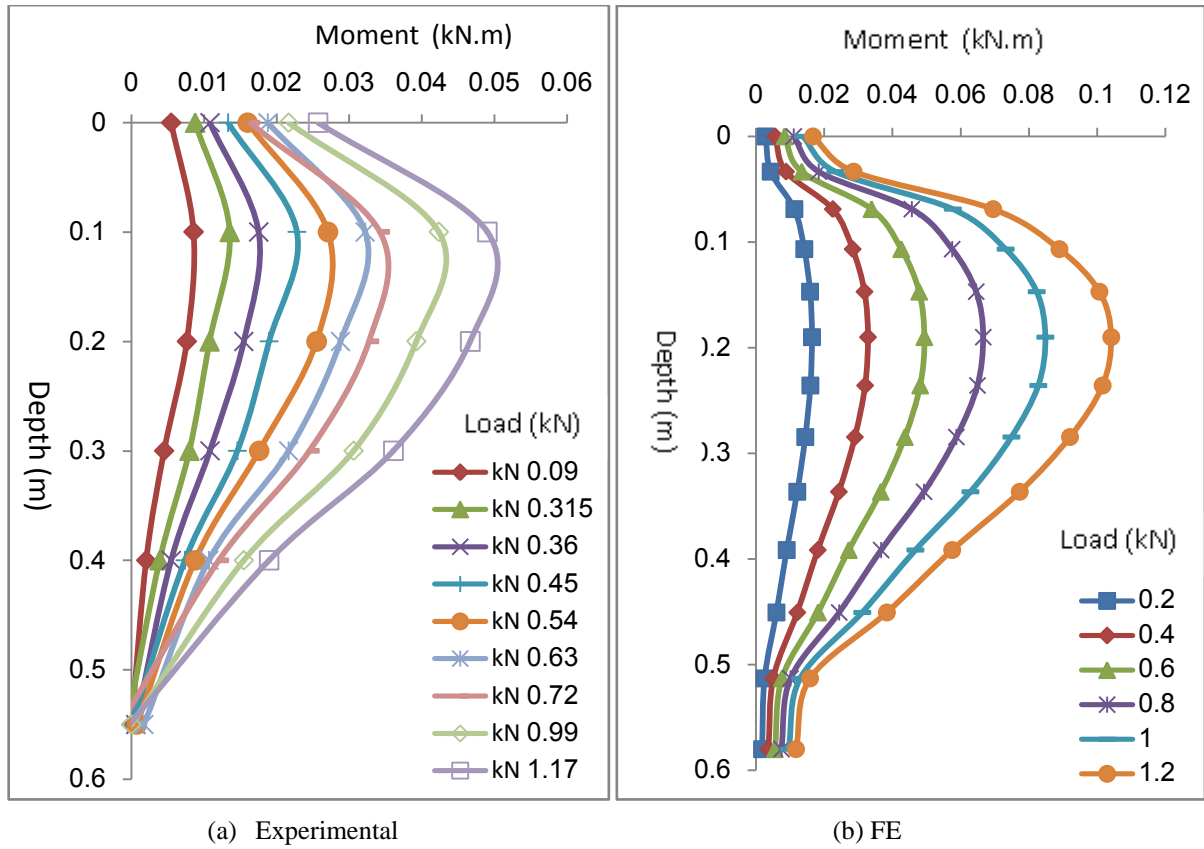


**Figure (8).** Moment-depth profiles for steel pile embedded in medium stiff clay (a) Experimental (b) FE

#### 4.1.2 Comparison with Elasticity Solutions

Two examples reported by Basu (2006) were analyzed using the FE analysis and the elasticity method represented by Poulos (1971). The results of pile deflection profile obtained from the FE model were compared with the results obtained from the elasticity method (Poulos, 1971).

Example 1 was a pile of 5m long, 0.5m diameter  $E_p = 25 * 10^6 \text{ kPa}$  and  $\mu_p = 0.2$  embedded in soil of  $E_s = 50 * 10^3 \text{ kPa}$  and  $\mu_s = 0.2$  subjected to lateral load of 294.5 kN.

Example 2 was illustrating a pile embedded in different soil layers. The pile length and diameters are 15 m and 0.6 m, respectively. The elastic modulus and Poisson's ratio are  $E_p = 24 * 10^6 \text{ kPa}$  and  $\mu_p = 0.2$ , respectively. the pile was subjected to lateral load of 300.0 kN. The soil parameters are presented in Table 2.

Using the theory of elasticity reference to Poulos (1971), equation (4) is used to calculate the pile head deflection at the ground surface ( $\rho$ ) for the above two piles. This deflection is compared with the results of the present FE model (Table 3).

$$\rho = I_{\rho H} \frac{H}{E_s L} + I_{\rho M} \frac{M}{E_s L^2} \quad (4)$$

where

$I_{\rho H}$  = The displacement influence factor for load only.

$I_{\rho M}$  = The displacement influence factor for moment only.

$I_{\rho H}$  and  $I_{\rho M}$  depends on the relative stiffness of the pile ( $K_R$ ) and L/d ratio.

H and M are the horizontal load and moment applied at the pile head.

$$K_R = \frac{E_p I_p}{E_s L^4} \quad (5)$$

Table 3 shows that the results of pile head deflection obtained by elastic method (Poulos, 1971) and the present FE model are the same.

**Table (2).** Soil parameters for example 2

Layer thickness	Elastic modulus $E_s$ (Mpa)	Poisson's ratio
2	20	0.35
5	35	0.25
8	50	0.2
5	80	0.15

**Table (3).** Comparison of pile deflection at the soil surface

Pile length (m)	Poulos (1971)	FE model
5	8.8	8.4
15	10.3	10.6

## 5. Parametric Study

The finite element program was used in a parametric study to investigate the effects of different vertical loads values and L/d ratios on the laterally loaded piles. The pile was embedded in medium stiff clay. The properties of the clay was presented in Table 1 above. The results were presented in terms of load-deflection curves at the pile head, load-maximum moment curves and the shear force along the length of the pile.

### 5.1 Effects of Vertical Load

A steel pile of diameter 250mm and L/d=20 embedded in medium stiff clay was used to perform a parametric study for the effects of different vertical loads values. The vertical load values considered were 20%, 40%, 60%, 80% and 100% of the ultimate vertical load capacity ( $V_u$ ). This ultimate vertical load capacity was obtained from a separate analysis for the same pile subjected to vertical load. The results are shown in Figures 10 to 12.

Figure 9 presents load-deflection curves for the vertical load. This curve shows a nonlinear pattern and the ultimate vertical load was taken to be 110 kN. Figure 10 presents load-deflection curves for laterally loaded steel pile with different vertical loads values. It is clear from this figure increasing the vertical load decreases the lateral

displacement which indicates some sort of fixity is occurred at the pile head due to the presence of the vertical load. Figure 11 presents load-maximum moment curves for laterally loaded steel pile with different vertical loads values. increasing the vertical load increases the moments this because the vertical stress are increased due to the axial loading. Therefore the presence of the vertical load decreases the lateral displacement and increases the moments. Figure 12 presents shear force diagram for laterally loaded pile without vertical load ( $V=0$ ) and with vertical load ( $V=V_u$ ). The shear force value is equal to the applied lateral load at the pile head and has a zero value at the pile tip. Moreover the depth of the point of the zero shear force ( $Dv$ ) did not change and equal to  $4.5d$  ( $d$ =pile diameter). This value is similar to the value that can be obtained by Briaud (1997) for infinitely long pile of length  $L > 3l_0$  by equation (6) and for short rigid pile ( $L \leq l_0$ ) by equation (7).

$$Dv = \frac{\pi}{4} l_0 \quad (6)$$

$$Dv = \frac{L}{3} \quad (7)$$

$$l_0 = \left( \frac{4EI}{K} \right)^{1/4} \quad (8)$$

$E$ = the elastic modulus of the pile ( $= 2.05 * 10^8 \text{ kN.m}^2$ )  
 $I$ = moment of inertia ( $\text{m}^4$ )

$K$ = soil spring constant ( $\text{kN.m}^2$ ) and it is the ratio of the soil pressure to the soil displacement.

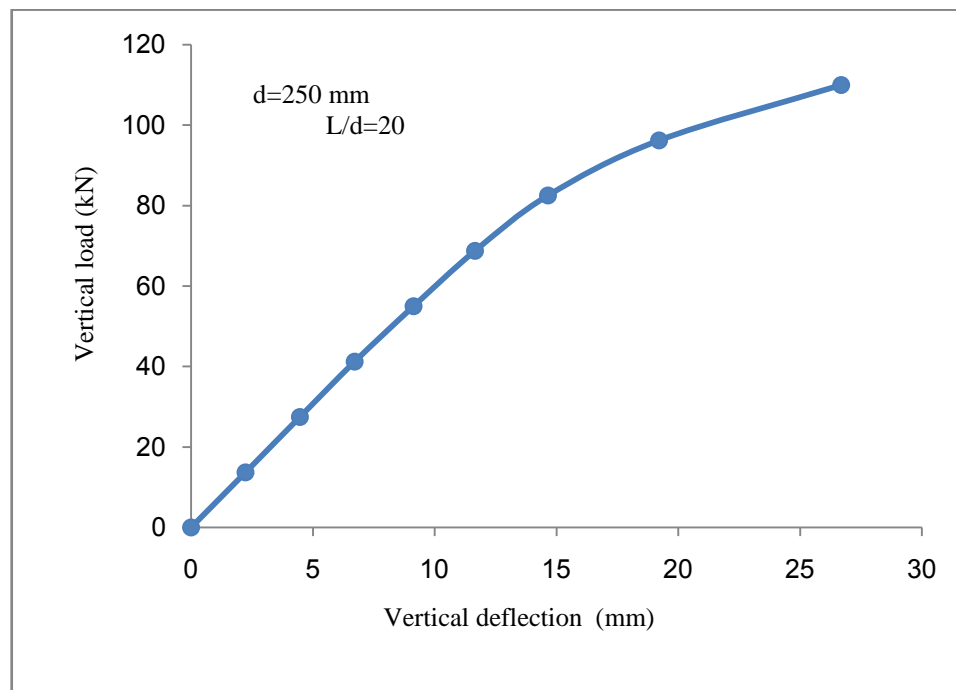


**Figure (9).** presents load-deflection curves for vertical load only

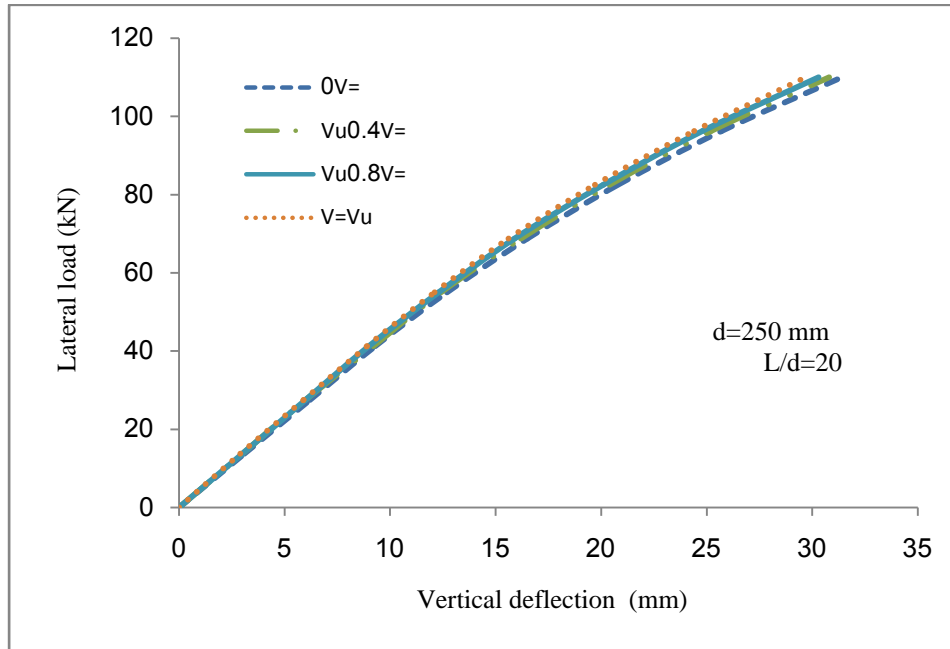


**Figure (10).** Load-deflection curves for laterally loaded steel pile with different vertical loads values

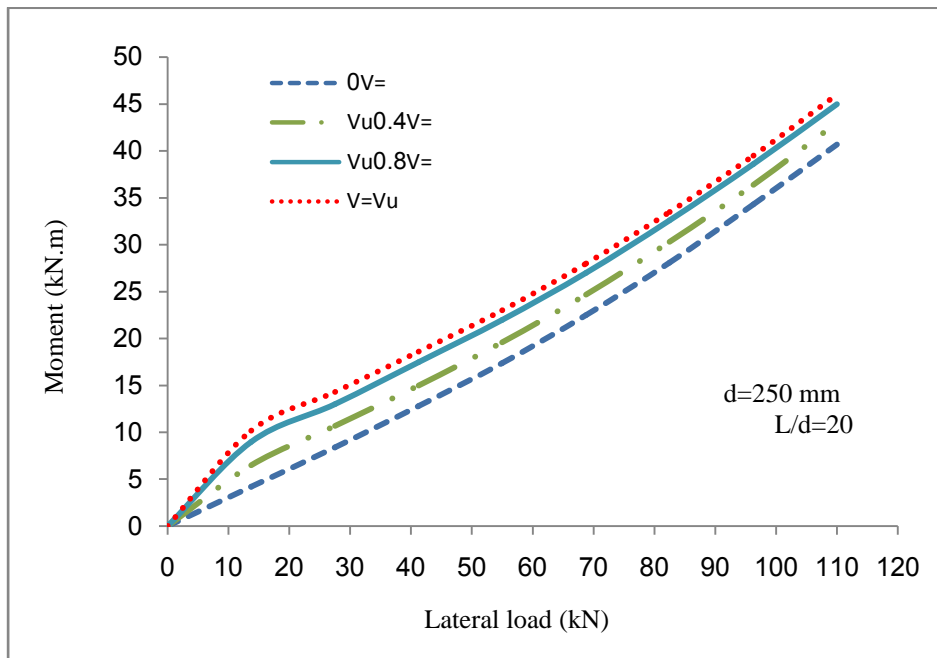


**Figure (11).** Load-maximum moment curves for laterally loaded steel pile with different vertical loads values

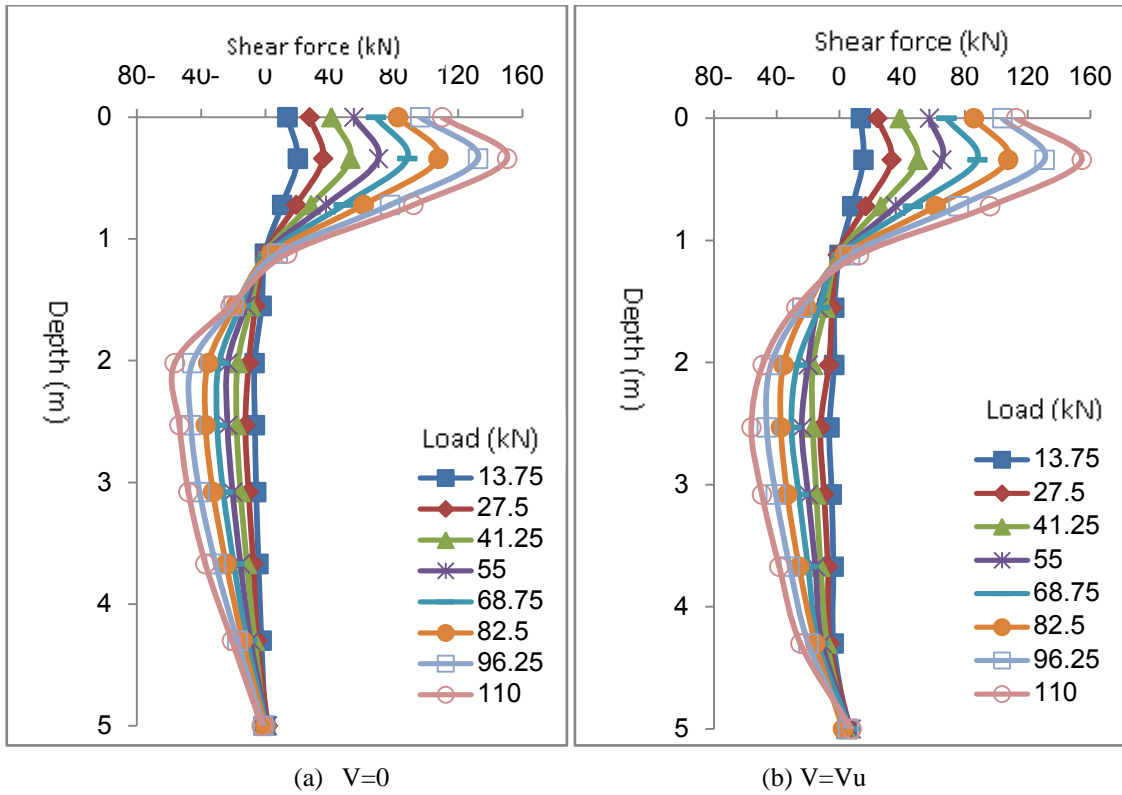


**Figure (12).** shear force diagram for laterally loaded pile#3 of  $L/d=20$  (a) without vertical load ( $V=0$ ) and (b) with vertical load ( $V=Vu$ )

## 5.2 Effects of $L/d$ Ratio

Three steel piles of different  $L/d$  ratios were used. The study shows the performance of laterally loaded pile embedded in medium stiff clay with and without vertical

load. Table 4 presents pile dimensions. Each pile was already subjected to its ultimate vertical capacity. The ultimate vertical load capacity was obtained from separate analysis for the same pile subjected to only vertical load.

**Table 4** Pile dimensions for the effect of  $L/d$  ratio

Pile#	Diameter (mm)	Pile length (m)	$L/d$ ratio	Surface area ( $m^2$ )	x-sectional area ( $m^2$ )
1	500	2.5	5	3.925	0.02
2	500	5	10	7.85	0.02
3	250	5	20	3.925	0.005

Figure 13 presents load-deflection curves for the three piles subjected to vertical load. It was seen that increasing  $L/d$  ratio by increasing pile length (piles#1 and 2) increased the ultimate vertical resistance of the pile while increasing  $L/d$  ratio by decreasing pile diameter (piles#2 and 3) decreased the ultimate vertical resistance of the pile. Figures 14 and 15 present load-deflection curves for laterally loaded steel piles. Figure 14 shows that the presence of the vertical load prior to the lateral load decreased the lateral deflection and the ultimate lateral resistance of the pile can not be considered at a deflection of  $0.1d$ . This happened because the vertical load exerted some sort of fixity to the pile head. Figure 15 shows that increasing  $L/d$  ratio by increasing pile length (piles#1 and 2) increased the ultimate lateral resistance of the pile while increasing  $L/d$  ratio by decreasing pile diameter (piles#2 and 3) decreased the ultimate lateral resistance of the pile.

Figures 16 to 19 present load-maximum moment curves for the three piles (Pile#1 to 3). Figures 16 to 18 show that the presence of the vertical load increased the maximum moment for all the three piles but did not change the position of the point of maximum bending moment. On the other hand increasing  $L/d$  ratio decreased the position of the point of maximum moment. Figure 19 shows that for both cases (with and without vertical load) increasing  $L/d$  ratio by increasing pile length (piles#1 and 2) increased the maximum moment of the pile while increasing  $L/d$  ratio by decreasing pile diameter (piles#2 and 3) decreased the maximum moment of the pile.

Figures 20 and 21 present the shear force diagram for pile#1 and 2 under lateral load with vertical load ( $V=Vu$ ) and without vertical load ( $V=0$ ). The shear force value was equal to the applied lateral load at the pile head and had a zero value at the pile tip. Moreover the depth of the point of the zero shear force ( $Dv$ ) did not

change with the presence of the vertical load. Table 4 presents the comparison between the depth of the zero shear force obtained from the present finite element analysis and that obtained by equations 6 and 7 reference to Briaud

(1997). This table shows similar results were obtained for the infinitely long pile of length  $L > 3l_0$  and for short pile of length  $L \leq l_0$ .

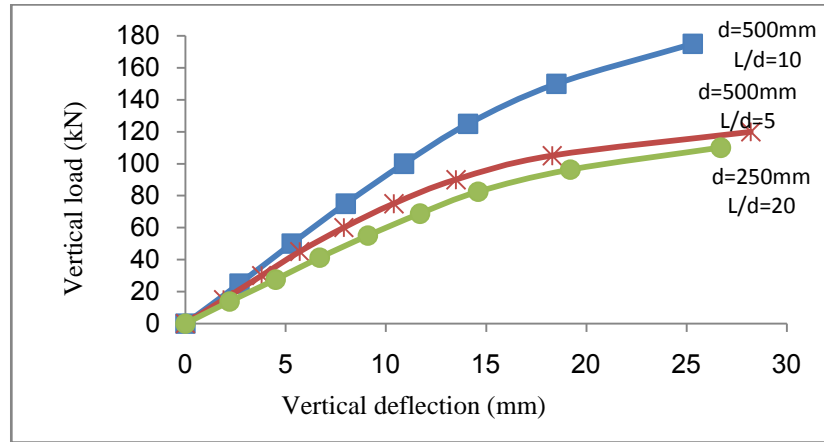


Figure (13). Load-deflection curves for vertical load

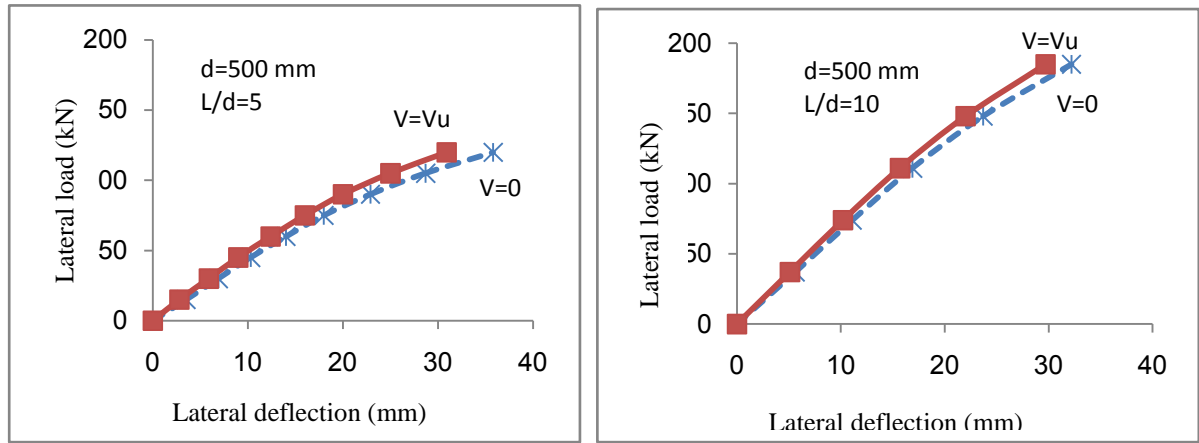


Figure (14). Load-deflection curves for lateral load with and without vertical load for (a)  $L/d=5$  and (b)  $L/d=10$

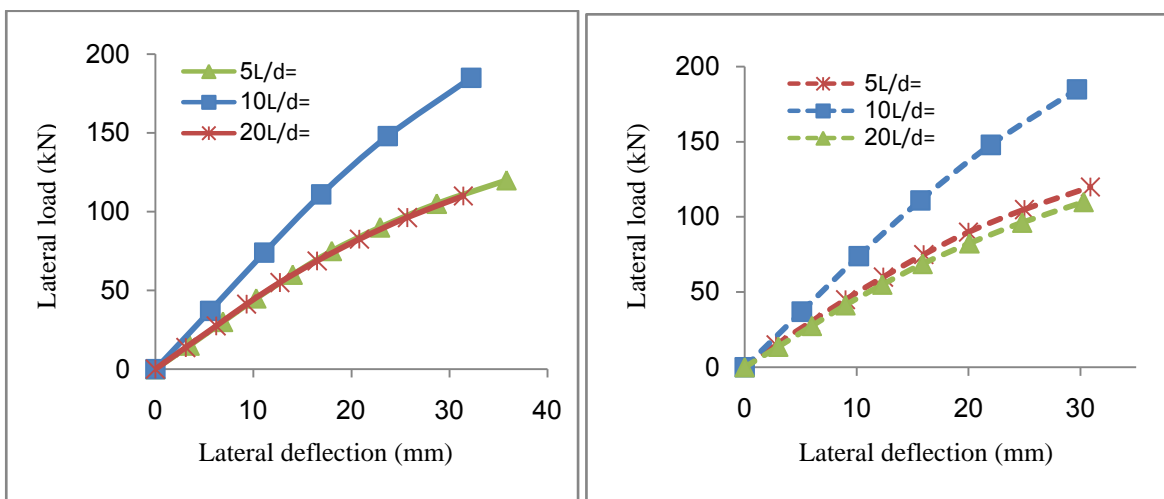
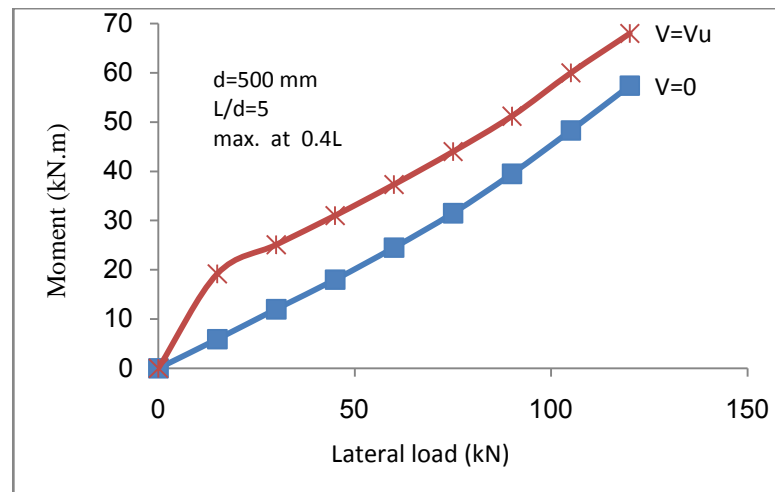
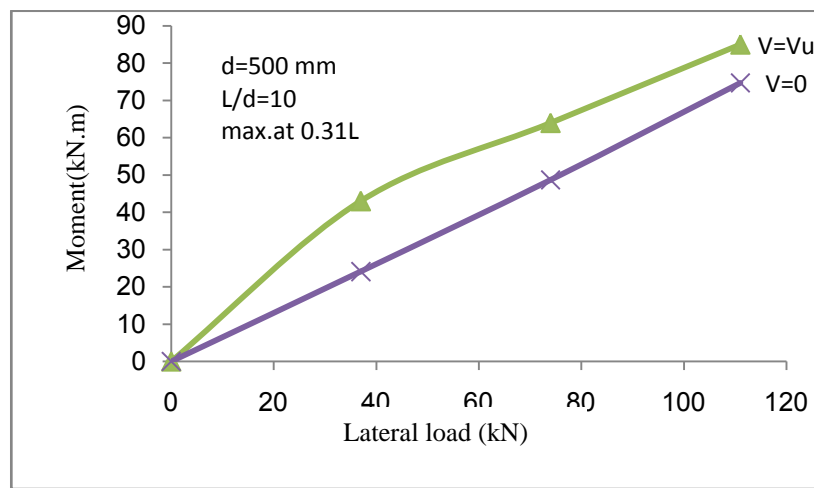


Figure (15). Load-deflection curves for steel pile with vertical load (a)  $V=0$  and without vertical load (b)  $V=Vu$



**Figure (16).** Load-maximum moment curves for pile#1 under lateral load with and without vertical load



**Figure (17).** Load-maximum moment curves for pile#2 under lateral load with and without vertical load

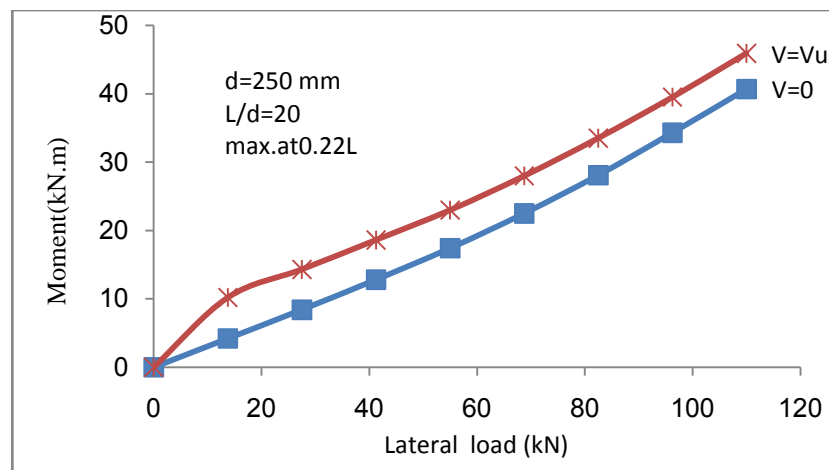


**Figure (18).** Load-maximum moment curves for pile#3 under lateral load with and without vertical load

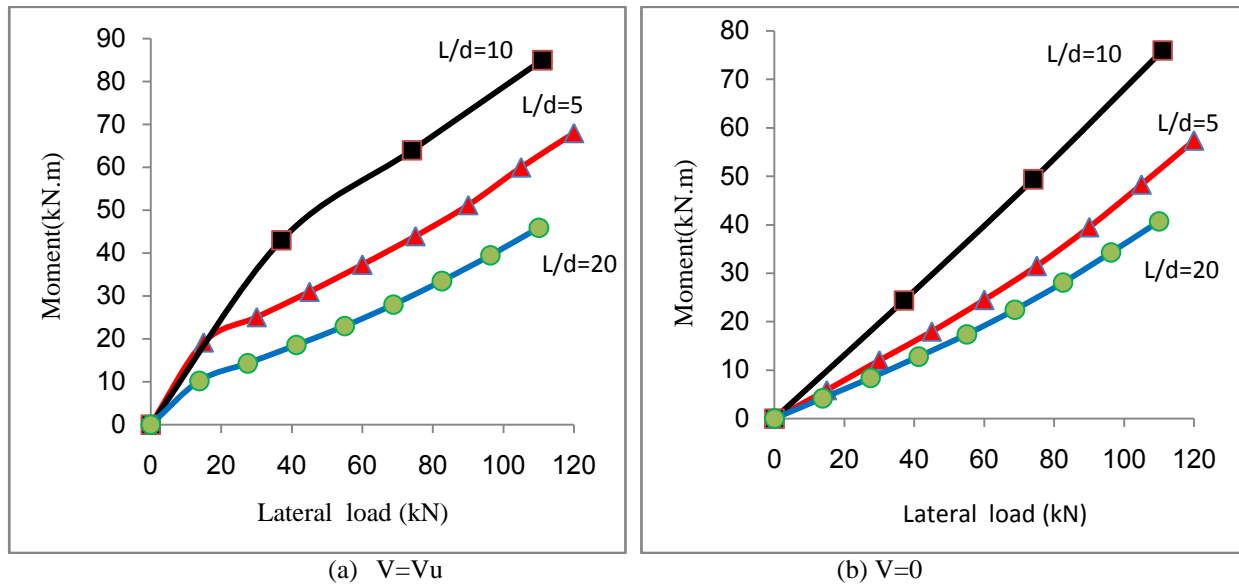


**Figure (19).** Load-maximum moment curve for steel piles of different  $L/d$  ratios with and without vertical load embedded in medium stiff clay

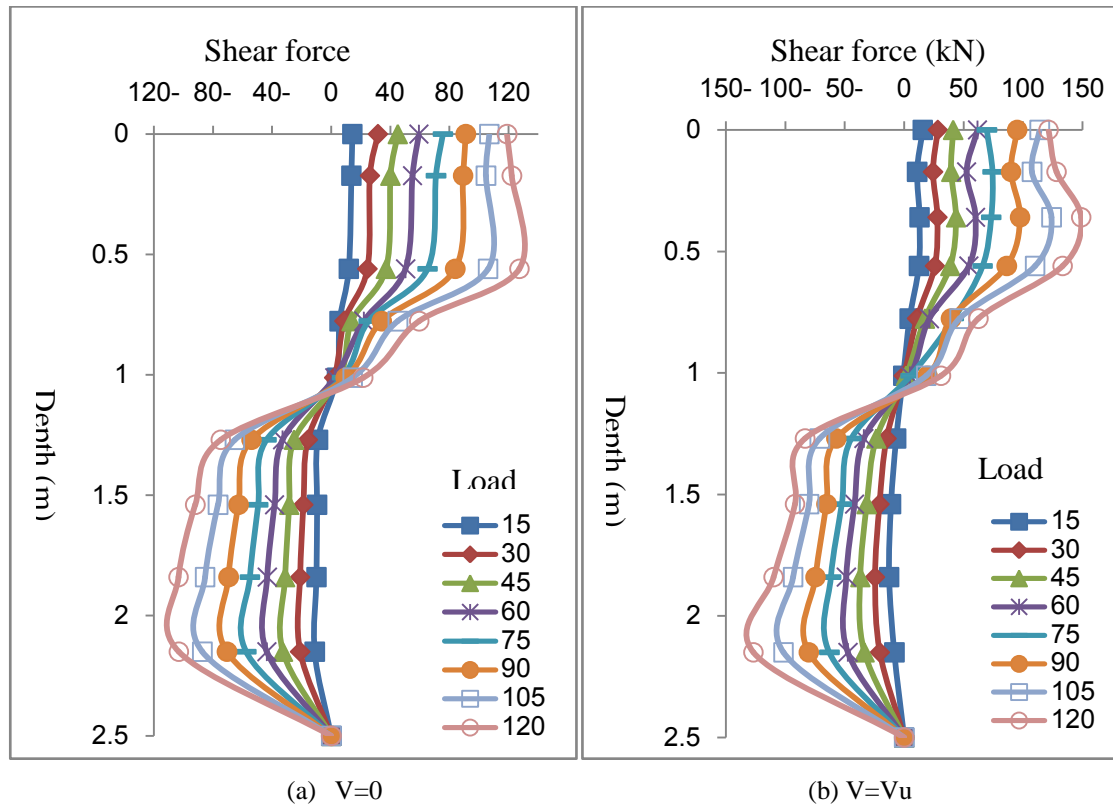


**Figure (20).** shear force diagram for pile#1 of  $L/d=5$  (a) without vertical load ( $V=0$ ) and (b) with vertical load ( $V=Vu$ )

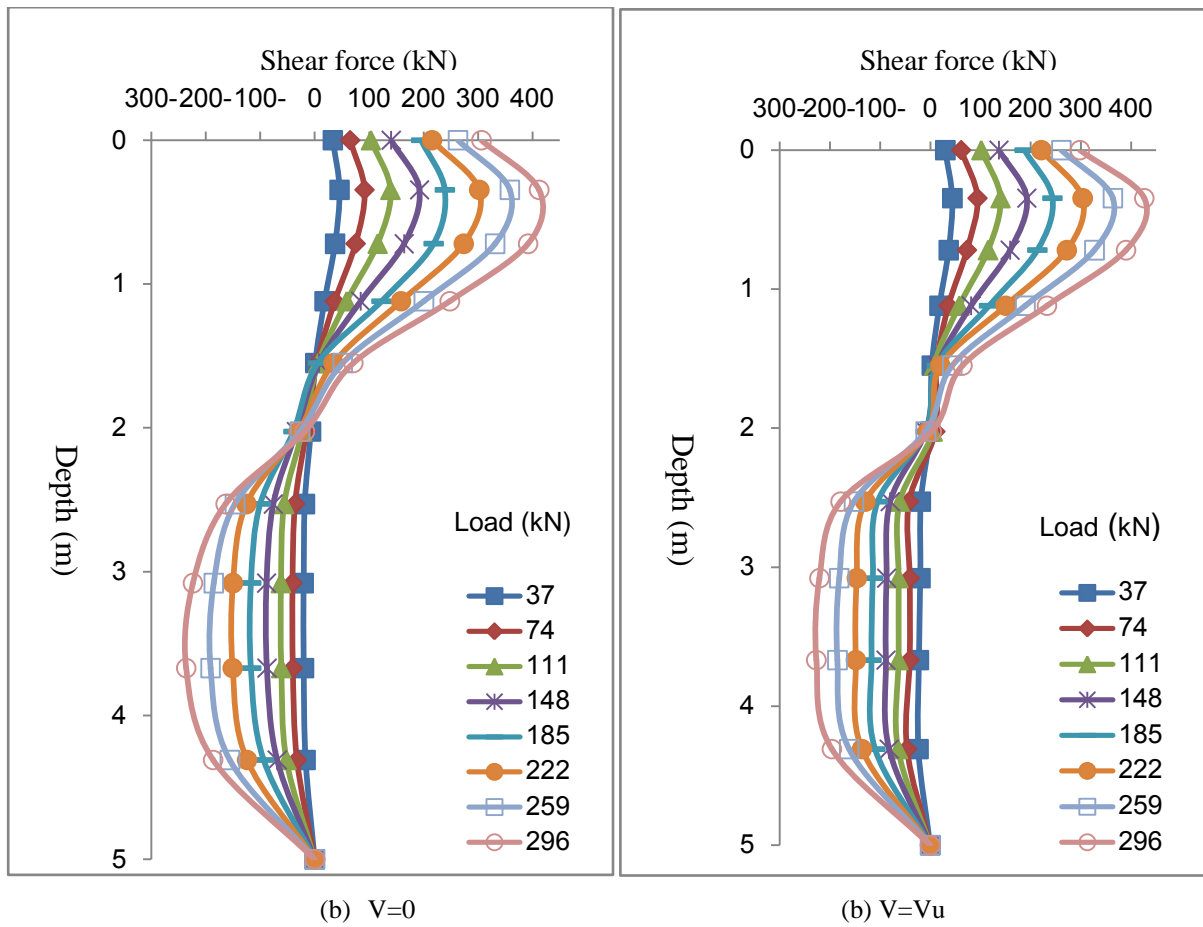


**Figure (21).** shear force diagram for pile#2 of  $L/d=10$  (a) without vertical load ( $V=0$ ) and (b) with vertical load ( $V=Vu$ )

**Table (4).** Comparison of depth of zero shear force

Pile#	Diameter (mm)	L/d ratio	$l_0$ ( $m^2$ )	L (m)	$Dv$ (m) (FE)	$Dv$ (m) (Briaud 1997)
1	500	5	5.6	2.5 ( $< l_0$ )	1.01	0.83
2	500	10	6.2	5 ( $< l_0$ )	1.60	1.67
3	250	20	1.53	5 ( $> 3l_0$ )	1.12	1.20

## 6. Conclusions

The performance of a laterally loaded single piles with and without vertical load was investigated by an experimental laboratory model tests and a theoretical finite element model. Also the effects of L/d ratio on the behavior of a laterally loaded pile with the presence of a vertical load was studied. The following points can be summarized:

- 1- The laboratory test and the FE model gave the same results for the load-deflection curves up to a deflection of 0.1d.
- 2- The results of the head deflection obtained by the FE are typical to that found by the elastic method.
- 3- Increasing the vertical load decreased the lateral deflection which indicated some sort of fixity was occurred at the pile head due to the presence of the vertical load. Also increasing the vertical load increased the maximum bending moments. Therefore the presence of the vertical load decreased the lateral deflection and increased the moments which leads to a significant reduction in the lateral resistance of the pile.
- 4- The presence of the vertical load did not change the position of the point of maximum bending moment.
- 5- Increasing L/d ratio by increasing pile length increased the ultimate vertical resistance of the pile while increasing L/d ratio by decreasing pile diameter decreased the ultimate vertical resistance of the pile.
- 6- For the laterally loaded pile with and without vertical load, increasing L/d ratio by increasing pile length increased the maximum moment of the pile while increasing L/d ratio by decreasing pile diameter decreased the maximum moment of the pile.
- 7- Increasing L/d ratio decreased the position of the point of maximum moment.
- 8- For the laterally loaded pile with and without vertical load, the shear force value was equal to the applied lateral load at the pile head and had a zero value at the pile tip. Moreover the depth of the point of the zero shear force ( $Dv$ ) did not change with the presence of the vertical load. The depth of the point of the zero shear force ( $Dv$ ) obtained from the finite element analysis was in good agreement with that obtained by Briaud (1997).

## REFERENCES

- [1] ABAQUS (2008). ABAQUS Standards User's Manual, Version 6.1, Hibbit, Karlsson and Sorensen, Inc.
- [2] Ahmed, M. M. and Ahmari, S., (2009). "Finite-Element Modeling of Laterally Loaded Piles in Clay". Proceedings of the Institutions of Civil Engineering, Geotechnical Engineering 163 Issue GE3, pp151-163.
- [3] Basu, D., (2006). "Analysis of Laterally Loaded Piles in Layered Soil". Ph. D. thesis Graduate School, Purdue University, U.S.A.
- [4] Briaud, Jean-Louis, (1997). "Simple Approach for Lateral Loads on Piles". Journal of Geotechnical and Geoenvironmental Engineering, © ASCE, Vol. 123, No. 10, pp. 958-964.
- [5] Dunnivant, T. W., and O'Neil, M. W., (1989), "Experimental  $p - y$  Model for Submerged, Stiff Clay". Journal of Geotechnical Engineering, © ASCE, Vol. 115, No. 1, pp. 95-114.
- [6] Elsharief, A. M. (1987) "Foundations on Expansive Soils". M. Sc. Thesis, BRRI, University of Khartoum, Sudan.
- [7] Fan, Chia-Cheng and Long, J.H., (2005). "Assessment of Existing Methods for Predicting Soil Response of Laterally Loaded Piles in Sand". Journal of Computers and Geotechnics, © Elsevier, 32 (2005), pp274-289.
- [8] Gabr, M. A.. (2002). " $P - y$  Analysis of Laterally Loaded Piles in Clay Using DMT". Journal of Geotechnical Engineering, © ASCE, Vol. 120, No. 5, pp. 816-837.
- [9] Hsiung Yun-mei, (2003). "Theoretical Elastic-Plastic Solution for Laterally Loaded Piles". Journal of Geotechnical and Geoenvironmental Engineering, © ASCE, Vol. 129, No. 6, pp. 475-480.
- [10] Kim, B. T., Kim, Nak-Kyung, Lee, W. J. and Kim, Y. S., (2004). "Experimental Load-Transfer Curves of Laterally Loaded Piles in Nak-Dong River Sand". Journal of Geotechnical and Geoenvironmental Engineering, © ASCE, Vol. 130, No. 4, pp. 416-425.
- [11] Karthigeyan, S., Ramakrishna, V.V.G.S.T. and Rajagopal, K., (2006). "Influence of Vertical Load on the Response of Piles in Sand". Journal of Computers and Geotechnics, © ELSEVIER, Vol. 33(2006), pp121-131.
- [12] Küükarslan, S. and Banarjee, P. K., (2004). "Inelastic Analysis of Pile-Soil Interaction". Journal of Geotechnical and Geoenvironmental Engineering, © ASCE, Vol. 130, No. 11, pp. 1152-1157.
- [13] Mayne, P. W., Kulhawy, F. H. and Trautmann, C. H., (1995). "Laboratory Modelling of Laterally-Loaded Drilled Shafts in Clay". Journal of Geotechnical Engineering, © ASCE, Vol. 121, No. 12, pp. 827-835.
- [14] Patra, N. R. and Pise, P. J., (2001). "Ultimate Lateral Resistance of Pile Groups in Sand". Journal of Geotechnical and Geoenvironmental Engineering, © ASCE, Vol. 127, No. 6, pp. 481-487.
- [15] Poulos, H. G. and Davis, E. H. (1980). "Pile Foundation Analysis and Design". Copyright © 1980, by John Wiley and Sons, Inc. New York.
- [16] Rajashree, S. S. and Sitharam, T. G., (2001). "Nonlinear Finite-Element Modeling of Battered Piles under Lateral Load". Journal of Geotechnical and Geoenvironmental Engineering, © ASCE, Vol. 127, No. 7, pp. 604-612.
- [17] Rao, S. N., Ramakrishna, V. G. S. T. and Rao, M. B., (1998). "Influence of Rigidity on Laterally Loaded Pile Groups in Marine Clay". Journal of Geotechnical and Geoenvironmental Engineering, © ASCE, Vol. 124, No. 6, pp. 542-549.
- [18] Reese, L. C., (1997). "Analysis of Laterally Loaded Piles in Weak Rock". Journal of Geotechnical and Geoenvironmental Engineering, © ASCE, Vol. 123, No. 11, pp. 1010-1017.
- [19] Sun, K., (1994). "Laterally Loaded Piles in Elastic Media". Journal of Geotechnical Engineering, © ASCE, Vol. 120, No. 8, pp. 1324-1344.

- [20] Sorochan, E. A. (1988). "Pile Foundation in Swelling Soils". Processing of 4<sup>th</sup> International Conference on Expansive Soils, Colorado, Vol. 2, PP. 845-849.
- [21] Wu, D., Broms, B. B. and Choa, V., (1998). "Design of Laterally Loaded Piles in Cohesive Soils Using  $P_y$  Curves". Japanese Geotechnical Society, Soils and Foundations ,Vol. 38, No. 2, pp. 17-26.
- [22] Yang, Ke (2006). " Analysis of Laterally Loaded Drilled Shafts in Rocks" Ph. D. Thesis presented to the Graduate Faculty of the University of Akron, U. S. A.